Geomechanics and Engineering, Vol. 2, No. 4 (2010) 281-302 281
DOI: http://dx.doi.org/10.12989/gae.2010.2.4.281

Response of rigid footing on reinforced granular fill over soft soil

K. Ramu[1] and Madhira R. Madhav*[2]

[1]*Department of Civil Engineering, JNT University College of Engineering, Kakinada, India - 533 003*
[2]*JNT University, 159, Road No. 10, Banajara Hills, Hyderabad 500 034, India*

(Received July 17, 2009, Accepted October 11, 2010)

Abstract. An extended model for the response of a rigid footing on a reinforced foundation bed on super soft soil is proposed by incorporating the rough membrane element into the granular bed. The super soft soil, the granular bed and the reinforcement are modeled as non-linear Winkler springs, non-linear Pasternak layer and rough membrane respectively. The hyperbolic stress-displacement response of the super soft soil and the hyperbolic shear stress-shear strain response of the granular fill are considered. The finite deformation theory is used since large settlements are expected to develop due to deformation of the super-soft soil. Parametric studies quantify the effect of each parameter on the stress-settlement response of the reinforced foundation bed, the settlement and tension profiles.

Keywords: geosynthetic reinforcement; finite deformation theory; granular bed; rigid footing; soft soil; hyperbolic response; settlement; tension.

1. Introduction

Ultimate bearing capacity of soft soil can be improved by placing a relatively rigid granular soil over it. It can be further improved by placing a reinforcement layer with in the granular layer. Extensive literature is available for the response of near surface loads on the reinforced foundation beds. The improvement in bearing capacity with reinforcement layers have been reported by Yang (1972), Binquet and Lee (1975b), Akinmusuru and Akinbolade (1981), Andrawes *et al.* (1983), Saran *et al.* (1985), Guido *et al.* (1985, 1986), Dembicki *et al.* (1986) and Milligan *et al.* (1986), Love *et al.* (1987), Purkayastha and Bhoumik (1988), Das (1989), Maheshwari *et al.* (2006), *etc.* Binquet and Lee (1975a and b) were the first to study the problem of bearing capacity of reinforced foundation bed systematically along with experimental validation. Basset and Last (1978) made a study of the soil below a footing, defined the strain field in terms of slip lines and suggested locations for the ideal placement of reinforcement.

Madhav and Poorooshasb (1988) proposed a model for the analysis of a footing on a reinforced granular bed. The subgrade soil, the granular bed and the reinforcement have been modelled by linear Winkler springs, a Pasternak shear layer and a rough membrane respectively. The results indicate that at small displacements, the contribution of shear layer far outweighs the effect of

*Corresponding author, Professor, E-mail: madhavmr@gmail.com

membrane action of the reinforcement in reducing the settlements of the reinforced soft soil. Ghosh and Madhav (1994) extended Madhav and Poorooshasb (1988) model by considering the non-linearity of soft soil and granular fill. Sukla and Chandra (1994) extended Madhav and Poorooshasb (1988) model by considering the pre-stress in the reinforcement layer and the compressibility of granular fill. Yin (1997a) presented an extension of Madhav and Poorooshasb (1988) model satisfying the compatibility of displacements at the interface of the fill and the reinforcing layer. Yin (1997b) further modified the model (Yin 1997a) by considering the non-linear responses of the soil and the fill.

All the presently available models are developed based on infinitesimal deformation theory. If the subgrade soil is very soft it undergoes large deformations especially at medium to large loads. In such cases, the infinitesimal deformation theory may not be appropriate nor give valid results. In this study, a new extended model is proposed incorporating a finite deformation approach to estimate the complete load-settlement response and the ultimate bearing capacity of a rigid footing resting on reinforced granular bed overlying super-soft clay. The hyperbolic stress-displacement response of the soft clay and the hyperbolic shear stress-shear strain response of the granular bed are considered. The undrained behaviour of the soft soil and the response of the granular fill are represented by elasto-plastic Winkler model and Pasternak shear layer respectively. Full mobilization of interface shear resistance at the interface of the fill and the reinforcement is assumed. Since the ground is very soft, very large settlements are expected during the placement of the granular fill and hence the problem is formulated as a moving boundary problem. For each incremental value of intensity of load, the settlement profile changes. The basic governing differential equations are developed by updating the profile for each increment of load intensity.

2. Proposed model and analysis: plane strain case

A rigid strip footing of width, $2B$, carrying an average intensity of load, q, resting on the reinforced granular fill of thickness, H, and width, $2L$, overlaying super-soft soil (Fig. 1(a)) is considered. The reinforcement (geosynthetic) layer is placed in the fill at a depth of H_t from the top of the fill, and is of length $2L_r$ ($L_r = L$). The above system is modeled (Fig. 1(b)) according to Madhav and Poorooshasb (1988) to consist of a shear layer, Winkler springs and a rough membrane to represent the granular fill, super-soft subgrade soil and a geosynthetic layer respectively.

The reinforced granular fill system is divided in to three elements (1), (2) and (3), for the purpose of analysis. The three elements are the fill above the reinforcement, the reinforcement and the fill below the reinforcement respectively. The forces in the elements (1), (2) and (3), are depicted in Figs. 2(a), (b) and (c) respectively. For an incremental average intensity of load, Δq, the governing equation for the equilibrium of element (1), using Pasternak shear layer concept can be written as

$$\Delta q = \Delta q_t + \frac{\partial \Delta N_x}{\partial x} \tag{1}$$

where Δq_t is the normal stress at the bottom of the element (1), *i.e.* above the reinforcement, $\partial \Delta N_x / \partial x$ is the variation of shear force along the vertical face of the element 1. The incremental shear force acting on the shear layer of thickness, H_t, is

$$\Delta N_x = \int_0^{H_t} \Delta \tau_{zx} dz \tag{2}$$

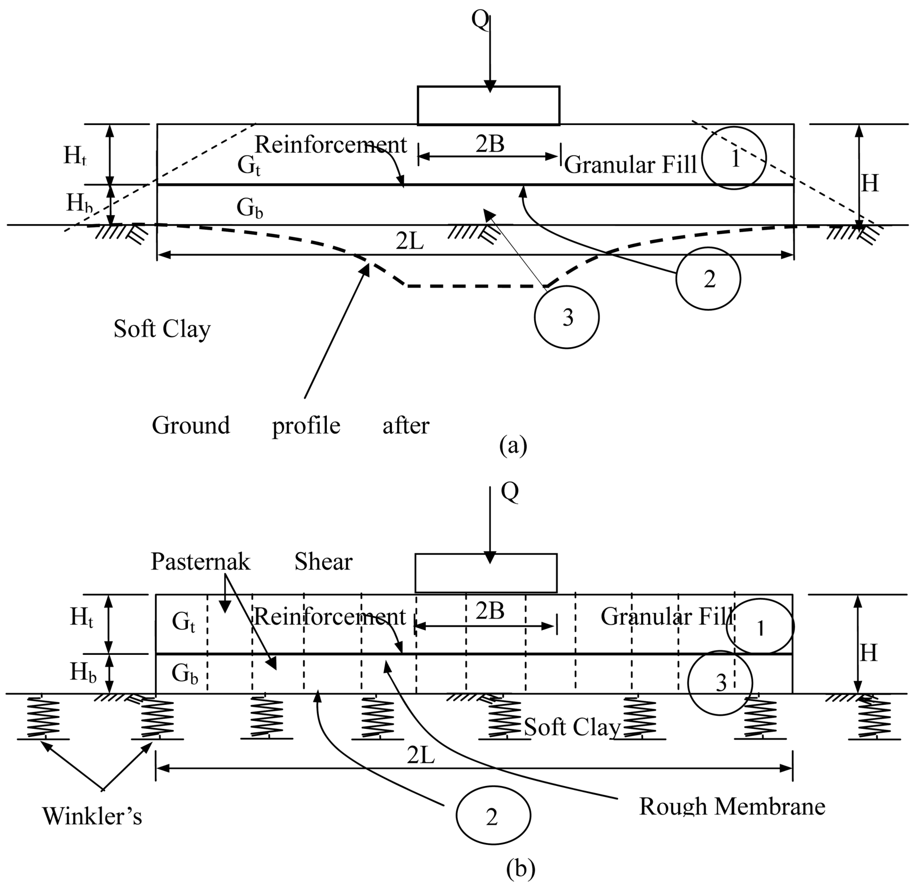

Fig. 1 (a) Rigid footing on a reinforced granular fill-super soft soil system and (b) the proposed model

Assuming incremental shear stress, $\Delta\tau_{zx}$, to be constant along the depth, H_t, of the granular fill, Eq. (2) becomes

$$\Delta N_x = \Delta\tau_{zx} H_t \tag{3}$$

The shear stress-shear strain response of the granular fill idealised as a hyperbolic relation (Kondner 1963) as shown in Fig. 3 and is expressed as

$$\tau_{zx} = \frac{G_t \gamma_{zx}}{\left(1 + \dfrac{G_t}{\tau_f}\gamma_{zx}\right)} \tag{4}$$

where the initial tangent modulus (shear modulus) is G_t while the asymptotic value of shear stress (ultimate shear resistance) is τ_f. γ_{zx} is the shear strain of the granular fill. Defining a non-linear parameter for the granular fill, β_g (= G_t/t_f) and differentiating Eq. (5) with respect to γ_{zx}, the incremental shear stress, Δt_{zx}, in the granular fill is

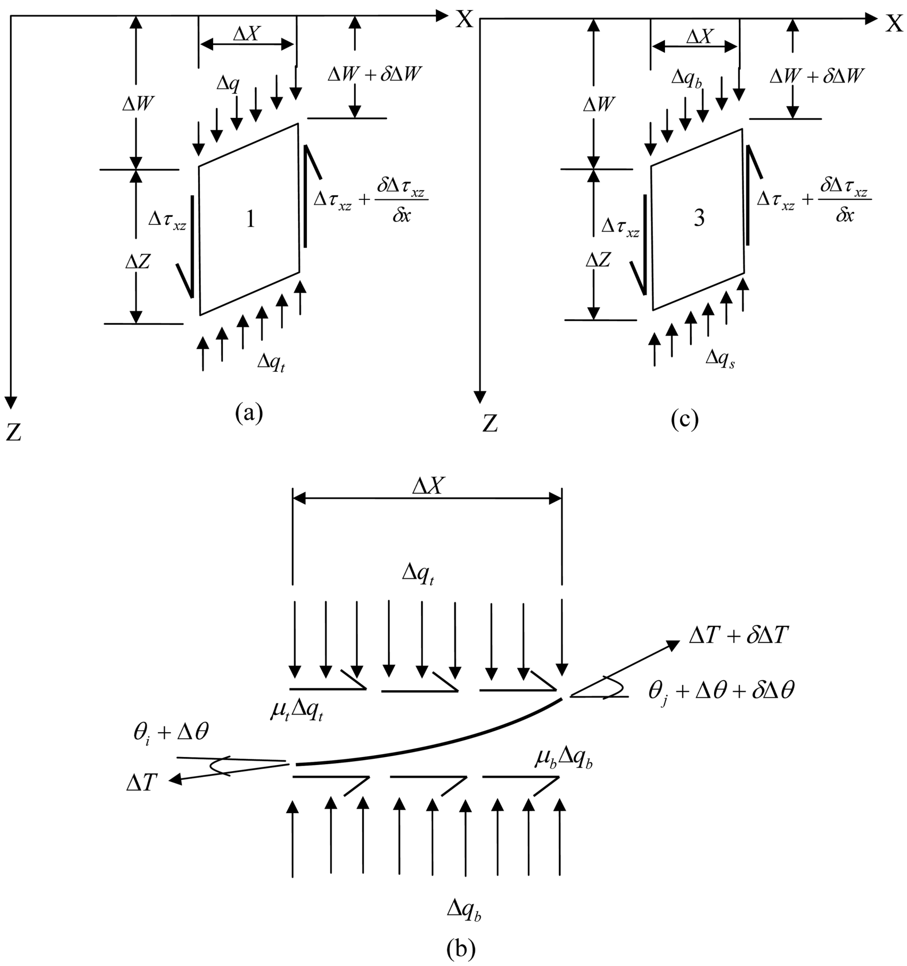

Fig. 2 Stresses in (a) the granular fill above reinforcement, element 1; (b) the reinforcement, element (2); (c) the granular fill below the reinforcement, element (3)

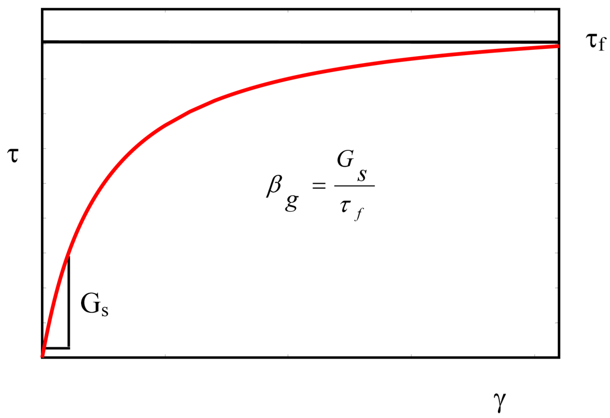

Fig. 3 Relation between shear stress and shear strain

$$\Delta\tau_{zx} = \frac{G_p \Delta\gamma_{zx}}{(1+\beta_g \gamma_{zx})^2} \tag{5}$$

where $\Delta\gamma_{zx}$ is the incremental shear strain of the granular fill. Substituting Eq. (5) in Eq. (3), one can get

$$\Delta N_x = \frac{G_t H_t}{(1+\beta_g \gamma_{zx})^2}\Delta\gamma_{zx} \tag{6}$$

The change in the displacement profile of an infinitesimal element of width, Δx, is shown in Fig. 4(a), when the uniform stress on the footing increases from 'q' to 'q+Δq'. The position of the infinitesimal element of length, Δx, (Fig. 4(b)), under the applied stress, q, is CD. The element displaces to EF when the stress becomes ($q + \Delta q$). Line EI is horizontal while EG is parallel to CD. As the applied stress increases to ($q + \Delta q$), the displacements of A and B increase respectively to $w(q + \Delta q, x)$ and $w(q + \Delta q, x + \Delta x)$. The shear strain now is $\gamma_{xz} + \Delta\gamma_{xz}$. From the triangle EFI

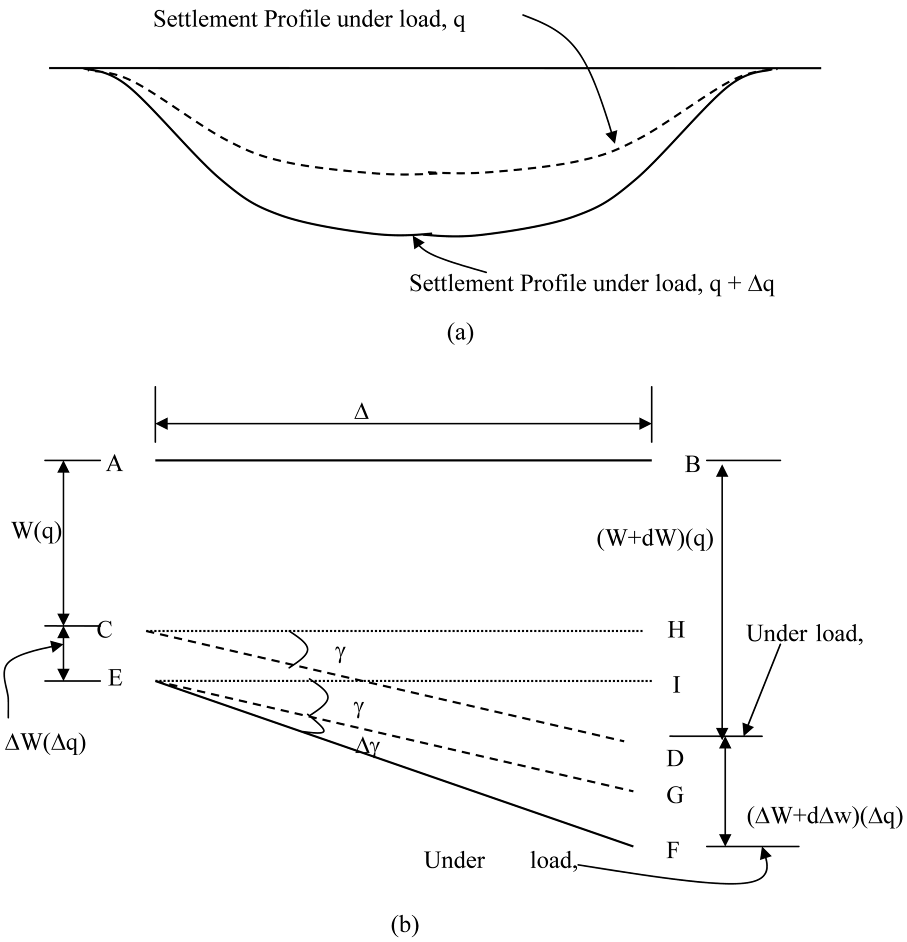

Fig. 4 (a) Displacement profile under incremental loads; (b) idealisation of displacement profiles

$$Tan(\gamma_{xz} + \Delta\gamma_{xz}) = \frac{\Delta w + d\Delta w}{dx} \tag{7}$$

where $d\Delta w$ is the increment in displacement of point B with respect to point A under the stress increment of Δq. Simplifying Eq. (7), one can get

$$Tan\Delta\gamma_{xz} \cong \Delta\gamma_{xz} = \frac{\frac{d\Delta w}{dx}}{\left(1 + \tan^2\gamma_{zx} + \tan\gamma_{zx}\frac{d\Delta w}{dx}\right)} \tag{8}$$

Substituting for $\Delta\gamma_{zx}$ from Eq. (8) in Eq. (6), one can get

$$\Delta N_x = \frac{G_t H_t}{(1 + \beta_g \gamma_{zx})^2} \frac{\frac{d\Delta w}{dx}}{\left(1 + \tan^2\gamma_{zx} + \tan\gamma_{zx}\frac{d\Delta w}{dx}\right)} \tag{9}$$

The variation in increment in shear force on the vertical face of the element (1) can be obtained by differentiating Eq. (9) with respect to x as

$$\frac{\partial \Delta N_x}{\partial x} = -G_t H_t \left[\frac{c_1\frac{d^2\Delta w}{dx^2} + c_2\frac{d\Delta w}{dx}\frac{d^2 w}{dx^2}}{(1 + \beta_g \gamma_{zx})^2 c_3^2}\right] \tag{10}$$

where $c_1 = 1 + \tan^2\gamma_{xz}$ $c_2 = \left\{\left(2\tan\gamma_{xz} + \frac{d\Delta w}{dx}\right) + \frac{2\beta_g}{(1 + \beta_g\gamma_{xz})}c_3\cos^2\gamma_{xz}\right\}$ and

$c_3 = \left(1 + \tan^2\gamma_{xz} - \tan\gamma_{xz}\frac{d\Delta w}{dx}\right)$.

Substituting Eq. (10) in Eq. (1), one gets

$$\Delta q = \Delta q_t - G_t H_t \left[\frac{c_1\frac{d^2\Delta w}{dx^2} + c_2\frac{d\Delta w}{dx}\frac{d^2 w}{dx^2}}{(1 + \beta_{gt}\gamma_{xz})^2 c_3^2}\right] \tag{11}$$

Similarly by considering the vertical force equilibrium of element 3 (Fig. 2(c), fill below the reinforcement layer), the governing equation is obtained as

$$\Delta q_s = \Delta q_b + G_b H_b \left[\frac{c_1\frac{d^2\Delta w}{dx^2} + c_2\frac{d\Delta w}{dx}\frac{d^2 w}{dx^2}}{(1 + \beta_{gb}\gamma_{zx})^2 c_3^2}\right] \tag{12}$$

where Δq_b and Δq_s are the vertical normal stresses at the top and bottom of the fill below the reinforcement, G_b, H_b and τ_{fb} are the initial shear modulus, thickness of the granular fill and the ultimate shear resistance respectively of the fill below the reinforcement.

Based on Winkler assumption, the vertical resistance, q_s, of the super-soft subgrade soil is

$$q_s = k_s w \tag{13}$$

where k_s and 'w' are the tangent subgrade modulus of super soft-soil and total displacement of the footing respectively. The stress-displacement response of the super-soft deposit is represented by a hyperbolic relation shown in Fig. 5 (Kondner 1963) as

$$q_b = \frac{k_s w}{\left(1 + \frac{k_s}{q_u} w\right)} \tag{14}$$

where 'q_b' is the vertical stress on top of the granular bed below the reinforcement, The initial tangent modulus (subgrade modulus) is k_s while the ultimate (asymptotic) value of stress (ultimate bearing capacity) is q_u. With non-dimensional parameter of super soft subgrade, $\beta_s = k_s B/q_u$, Eq. (19) becomes

$$q_s = \frac{k_s w}{\left(1 + \beta_s \frac{w}{B}\right)} \tag{15}$$

Differentiating Eq. (15) with respect to w, the increment in resistance, Δq_b, of the super-soft soil is

$$\Delta q_b = \frac{k_s \Delta w}{(1 + \beta_s w)^2} \tag{16}$$

where Δw is the incremental settlement, $q_u = c_u N_c$, – the ultimate bearing capacity of the footing on super-soft ground, c_u – undrained strength of soft soil and N_c – the bearing capacity factor.

Considering the reinforcement in the reinforced granular fill, *i.e.* element (2), (Fig. 2(b)), the horizontal force equilibrium requires,

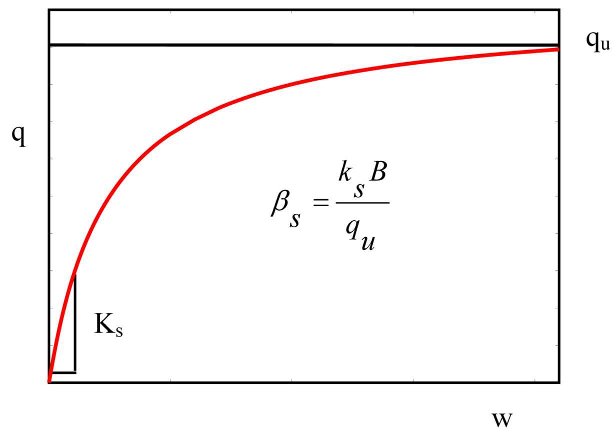

Fig. 5 Relation between intensity of load and settlement

$$\frac{d\Delta T}{dx}\cos(\theta+\Delta\theta) - \Delta T\sin(\theta+\Delta\theta)\frac{d\Delta\theta}{dx} = -(\mu_t\Delta q_t + \mu_b\Delta q_b) - (\Delta c_{at} + \Delta c_{ab}) \tag{17}$$

where θ and $\Delta\theta$ are the inclinations of the deformed shape of the granular fill at the end of the previous lift and the incremental inclination of the deformed element caused by the incremental load, Δq, respectively. μ_t and Δc_{at} are the frictional and adhesive resistances respectively at the interface between the top granular fill and the reinforcement, μ_b and Δc_{ab} are the frictional and adhesive resistances respectively at the interface of the bottom granular fill and the reinforcement, ΔT is the increase in tension in the reinforcement with the increase in intensity of load, Δq. Similarly, from the vertical equilibrium of the forces in the reinforcement element (2), one gets

$$\frac{d\Delta T}{dx}\sin(\theta+\Delta\theta) + \Delta T\cos(\theta+\Delta\theta)\frac{d\Delta\theta}{dx} = (\Delta q_t - \Delta q_b) \tag{18}$$

Multiplying Eq. (17) by $\cos(\theta+\Delta\theta)$ and Eq. (18) by $\sin(\theta+\Delta\theta)$ and adding, one obtains

$$\frac{d\Delta T}{dx} = (\Delta q_t - \Delta q_b)\sin(\theta+\Delta\theta) - (\mu_t\Delta q_t + \mu_b\Delta q_b + \Delta c_{at} + \Delta c_{ab})\cos(\theta+\Delta\theta) \tag{19}$$

Similarly multiplying Eq. (17) by $\sin(\theta+\Delta\theta)$ and Eq. (18) by $\cos(\theta+\Delta\theta)$ and subtracting the former from the latter, the following equation can be obtained

$$\Delta T\frac{d\Delta\theta}{dx} = \sin(\theta+\Delta\theta)\{\mu_t\Delta q_t + \mu_b\Delta q_b + \Delta c_{at} + \Delta c_{ab}\} + \cos(\theta+\Delta\theta)\{\Delta q_t - \Delta q_b\} \tag{20}$$

Rearranging the terms of Eq. (19), one gets

$$\frac{d\Delta T}{dx} = -\{\mu_t\cos(\theta+\Delta\theta) - \sin(\theta+\Delta\theta)\}\Delta q_t - \{\mu_b\cos(\theta+\Delta\theta) + \sin(\theta+\Delta\theta)\}\Delta q_b - \cos(\theta+\Delta\theta)\{\Delta c_{at} + \Delta c_{ab}\} \tag{21}$$

Rearranging the terms of Eq. (20), one gets

$$\Delta T\frac{d\Delta\theta}{dx} = -\{\mu_t\sin(\theta+\Delta\theta) + \cos(\theta+\Delta\theta)\}\Delta q_t - \{\mu_b\sin(\theta+\Delta\theta) - \cos(\theta+\Delta\theta)\}\Delta q_b \tag{22a}$$

or

$$\Delta q_t = \left\{\frac{1-\mu_b\tan(\theta+\Delta\theta)}{1+\mu_t\tan(\theta+\Delta\theta)}\right\}\Delta q_b - \Delta T\frac{d\Delta\theta}{dx}\frac{1}{\cos(\theta+\Delta\theta) + \mu_t\sin(\theta+\Delta\theta)} \tag{22b}$$

Substituting Eqs. (11) and (12) in Eq. (21), one gets

$$\begin{aligned}\frac{d\Delta T}{dx} = &-(\mu_t\cos(\theta+\Delta\theta) - \sin(\theta+\Delta\theta))\left[\Delta q + G_tH_t\left(c_2\frac{d^2\Delta w}{dx^2} - \frac{d\Delta w}{dx}(c_3+c_4)\frac{d^2\Delta w}{dx^2}\right)/c_1^2\right] \\ &-(\mu_b\cos(\theta+\Delta\theta) - \sin(\theta+\Delta\theta))\left[\frac{k_s\Delta w}{(1+\beta_s w/B)^2} + G_bH_b\left(c_2\frac{d^2\Delta w}{dx^2} - \frac{d\Delta w}{dx}(c_3+c_4)\frac{d^2\Delta w}{dx^2}\right)/c_1^2\right] \\ &-\cos(\theta+\Delta\theta)\{\Delta c_{at} + \Delta c_{ab}\}\end{aligned} \tag{23}$$

Eq. (23) relates the variation of the incremental tensile force in the reinforcement to the incremental load of intensity, Δq. The corresponding equation by infinitesimal deformation theory

(Ramu 2001) is

$$\frac{dT}{dx} = -(\mu_t \cos\theta - \sin\theta)\left[q + \frac{G_t H_t}{\left(1+\beta_g \frac{dw}{dx}\right)^2} \frac{d^2 w}{dx^2} \right] - (\mu_b \cos\theta + \sin\theta)\left[\frac{k_c w}{1+\beta_s \frac{w}{B}} \right] - (C_{at} + C_{ab})\cos\theta \tag{24}$$

Substituting Eqs. (11) and (12) in Eq. (22b), and simplifying, the expression becomes

$$\begin{aligned}\Delta q = &-\left[\left(G_t H_t + G_b H_b \left\{\frac{1+\mu_b \tan(\theta+\Delta\theta)}{1-\mu_t \tan(\theta+\Delta\theta)}\right\}\right)\left(c_2 \frac{d^2 \Delta w}{dx^2} - \frac{d\Delta w}{dx}(c_3+c_4)\frac{d^2\Delta w}{dx^2}\right)/c_1^2\right] \\ &-\left\{\frac{\Delta T \cos^2 \Delta\gamma_{zx}}{\cos(\theta+\Delta\theta) - \mu_t \sin(\theta+\Delta\theta)}\right\}\left(c_2 \frac{d^2\Delta w}{dx^2} - \frac{d\Delta w}{dx} c_3 \frac{d^2 \Delta w}{dx^2}\right)/c_5^2 \\ &+ \frac{k_s \Delta w}{(1+\beta_s w/B)^2}\left\{\frac{1+\mu_b \tan(\theta+\Delta\theta)}{1-\mu_t \tan(\theta+\Delta\theta)}\right\}\end{aligned} \tag{25}$$

The corresponding equation by the infinitesimal theory is

$$\begin{aligned} q = &\left(\frac{1-\mu_b \cos\theta}{1+\mu_t \cos\theta}\right)\frac{k_s w}{1+\beta_s w/B} - \frac{\tan\theta}{1+\mu_t\cos\theta}(C_{at}+C_{ab}) \\ &- \left[\frac{G_t H_t}{\left(1+\beta_g \frac{dw}{dx}\right)^2} + \frac{G_b H_b}{\left(1+\beta_g \frac{dw}{dx}\right)^2}\left(\frac{1-\mu_b \cos\theta}{1+\mu_t \cos\theta}\right) + \frac{T\cos\theta}{1+\mu_t \cos\theta}\right]\frac{d^2 w}{dx^2}\end{aligned} \tag{26}$$

Normalising the terms with $q^* = q/k_s B$, $W = w/B$, $X = x/B$, $\Delta X = \Delta x/B$, $\Delta W = \Delta w/B$, $\Delta q^* = \Delta q/k_s B$, $\Delta T^* = \Delta T/k_s B^2$ and $G_t^* = G_t H_t/k_s B^2$, $G_b^* = G_b H_b/k_s B^2$, Eqs. (25) and (23) become

$$\begin{aligned}\Delta q^* = &-\left[\left(G_t^* + G_b^* \left\{\frac{1+\mu_b \tan(\theta+\Delta\theta)}{1-\mu_t \tan(\theta+\Delta\theta)}\right\}\right)\left(c_2 \frac{d^2 \Delta W}{dX^2} - \frac{d\Delta W}{dX}(c_3^*+c_4^*)\frac{d^2 W}{dX^2}\right)/(c_1^*)^2\right] \\ &-\left\{\frac{\Delta T \cos^2 \Delta\gamma_{zx}}{\cos(\theta+\Delta\theta) - \mu_t \sin(\theta+\Delta\theta)}\right\}\left(c_2 \frac{d^2\Delta W}{dX^2} - \frac{d\Delta W}{dX} c_3^* \frac{d^2 W}{dX^2}\right)/(c_5^*)^2 \\ &+ \frac{\Delta W}{(1+\beta_s W)^2}\left\{\frac{1+\mu_b \tan(\theta+\Delta\theta)}{1-\mu_t \tan(\theta+\Delta\theta)}\right\}\end{aligned} \tag{27}$$

and

$$\begin{aligned}\frac{d\Delta T^*}{dX} = &-(\mu_t \cos(\theta+\Delta\theta) - \sin(\theta+\Delta\theta))\left[\Delta q^* + G_t^*\left(c_2 \frac{d^2\Delta W}{dX^2} - \frac{d\Delta W}{dX}(c_3^*+c_4^*)\frac{d^2 W}{dX^2}\right)/(c_1^*)^2\right] \\ &-(\mu_b \cos(\theta+\Delta\theta) - \sin(\theta+\Delta\theta))\left[\frac{\Delta W}{(1+\beta_s W)^2} + G_b^*\left(c_2 \frac{d^2\Delta W}{dX^2} - \frac{d\Delta W}{dX}(c_3^*+c_4^*)\frac{d^2 W}{dX^2}\right)/(c_1^*)^2\right]\end{aligned} \tag{28}$$

where $c_5^* = (1 + \tan^2\gamma_{zx} - \tan\gamma_{zx}\, d\Delta W/dX)$; $c_1^* = c_5^*(1 + \beta_g\gamma_{zx})$; $c_3^* = (2\tan\gamma_{xz} - d\Delta W/dX)$, $c_4 = 2\beta_g\, c_5^* \cos^2\theta/(1 + \beta_g\gamma_{zx})$.

Four boundary conditions are required to solve the above two partial differential equations, (Eqs. (27) and (28)). They are at $x = 0$ or $X = 0$, the incremental displacement and the incremental tension are maximum as the slope of the settlement profile at this point is zero. *i.e.*

$$d\Delta w/dx = 0 \quad \text{or} \quad d\Delta W/dX = 0 \tag{29a}$$

and the slope of the tension curve also is zero. *i.e.*

$$d\Delta T/dx = 0 \quad \text{or} \quad d\Delta T^*/dX = 0 \tag{29b}$$

Similarly at $x = L$ or $X = L^*$, *i.e.* at the edge of the reinforced granular fill, the slope of the settlement profile is zero (no shear layer effect), *i.e.*

$$d\Delta w/dx = 0 \quad \text{or} \quad d\Delta W/dX = 0 \tag{29c}$$

and the tension is zero at the free edge (the free end of the reinforcement). Hence

$$\Delta T = 0 \quad \text{or} \quad \Delta T^* = 0 \tag{29d}$$

3. Numerical experimentation

Eqs. (27) and (28) are coupled and non-linear and hence need to be solved numerically to evaluate the settlement profile and the tension in the reinforcement at any point. Eqs. (27) and (28) are solved iteratively for each incremental displacement ΔW, of the rigid footing, with the boundary conditions (Eqs. 29) to obtain the incremental average intensity of load, Δq^*. These incremental average intensity of loads are summed up to get the total load as

$$q_i^*(W + \Delta W) = q_i^*(W) + \Delta q_i^*(\Delta W) \quad \text{for } 0 < i < nt + 1 \tag{30}$$

where $q_i^*(W)$ and $q_i^*(W + \Delta W)$ are the normalised total average intensity of loads under the settlements, W and $W + \Delta W$ respectively. Similarly, the increments in tensions are summed up to get the total mobilized tension as

$$T_i^*(q + \Delta q) = T_i^*(q) + \Delta T_i^* \quad \text{for } 0 < i < nt + 1 \tag{31}$$

where $T_i(q^*)$ and $T_i(q^* + \Delta q^*)$ are the normalised tensions in the reinforcement under the settlements, W and $W + \Delta W$ respectively.

For the rigid footing, uniform incremental displacements, ΔW_0, are specified over the width of the footing. In the first iteration Eq. (27) is solved assuming the incremental tension, ΔT_i, to be zero, thus determining the incremental average intensity of load, Δq^*. The tensions, ΔT_i, are then evaluated by solving Eq. (28) with the above computed average intensity of load, Δq^*. In the subsequent iterations the previously evaluated tensions and average intensity of loads (*i.e.* at $(k-1)^{th}$ iteration) are substituted and new values (*i.e.* at k^{th} iteration) are obtained till the old and new values converge. The convergence criteria for incremental average intensity of load and incremental tensions are as follows

$$\frac{\left|\Delta q_i^{*k} - \Delta q_i^{*k-1}\right|}{\Delta q_i^{*k}} \le 0.000005 \text{ and} \tag{32a}$$

$$\frac{\left|\Delta T_i^{k} - \Delta T_i^{k-1}\right|}{\Delta T_i^{k}} \le 0.000005 \tag{32b}$$

4. Convergence study

The quantities q_i^* and T_i^* are estimated by varying the number of elements, n, into which the half width of the footing is divided. A convergence study is carried out to minimise the numerical error, by varying the discretisation of the domain. The number of elements, n, is varied from 10 to 100. The results did not vary much except at large settlements and even at large settlement ($W \ge 1.0$) the solution converges for the number of elements, n, equal to or greater than 50. Hence the number of elements, 'n', into which the loaded region, B, is decretised is made equal to 50 in the subsequent analysis. A further study was then carried out with $n = 50$ but by varying the incremental settlement, ΔW^*. The accuracy of the results improved with decreasing values of ΔW^*. However, for $\Delta W^* < 0.0001$, no perceptible change in normalised settlement, W, was observed. Therefore all further analyses have been carried out with $n = 50$ and $\Delta W^* = 0.0001$.

5. Results and discussion

Only half the width of the reinforced zone is considered for the analysis considering symmetry of the applied load and of the reinforced zone. Half width of the loading, B, and the half width of the reinforced zones, L are divided into 'n' and 'nt' number of elements of equal length, Δx, as shown in Fig. 6. The loading boundary conditions are

$\Delta q_i = \Delta q$ for $0 < i \le n$

$\Delta q_i = \Delta q/2.0$ for $i = n + 1$

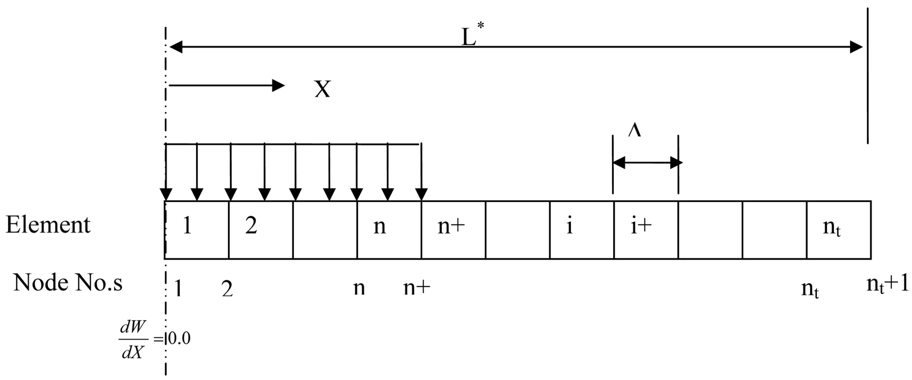

Fig. 6 Descritisation of the load and the reinforced granular bed

Table 1 Typical values for the modulus of subgrade reaction, k_s, (kN/m^3) for normally consolidated clay (after Terzaghi 1955)

Type of soil	Modulus of subgrade reaction, k_s
Very soft clays	1560 kN/m^3
Stiff clays	7800 kN/m^3

$$\Delta q_i = 0 \qquad \text{for } n+1 < i \leq nt+1$$

Settlements of the reinforced foundation bed and tension developed in the reinforcement layer, under rigid loading are studied through a parametric study, for the following ranges of modulus of subgrade reaction, k_s, of soft ground shown in Table 1. The shear modulus of the granular fill is varied from 1,500 to 50,000 kN/m^2.

The interface friction angle between the reinforcement and the granular fill varied from 0 to 45^o (smooth to perfectly rough membrane). Normalised settlements of the reinforced foundation bed and the normalized tension developed in the reinforcement layer, under uniform loading are studied through a parametric study, for the following ranges of non-dimensional parameters $G_t^* = G_b^* = 0.05$ to 1.0; $\beta_s = 5$ to 100; $\beta_g = 5$ to 50; $q^* = 0.01$ to 0.2, $\mu_t = \mu_b = 0$ (smooth) to 1.0 (fully rough) membrane.

The modulus of subgrade reaction, k_s, the stiffness of the granular bed, G_t, and the ultimate bearing resistance, q_u, and the interface bond resistance between the reinforcement and the fill, are the basic parameters which affect the physics of the problem and hence considered as they control the overall performance of the reinforced granular bed on soft ground to applied loads. The normal working ranges of the above parameters are estimated based on which the ranges of the normalized parameters worked out for the parametric study.

The variation of settlement along the width of the reinforced sand bed from its center by the both

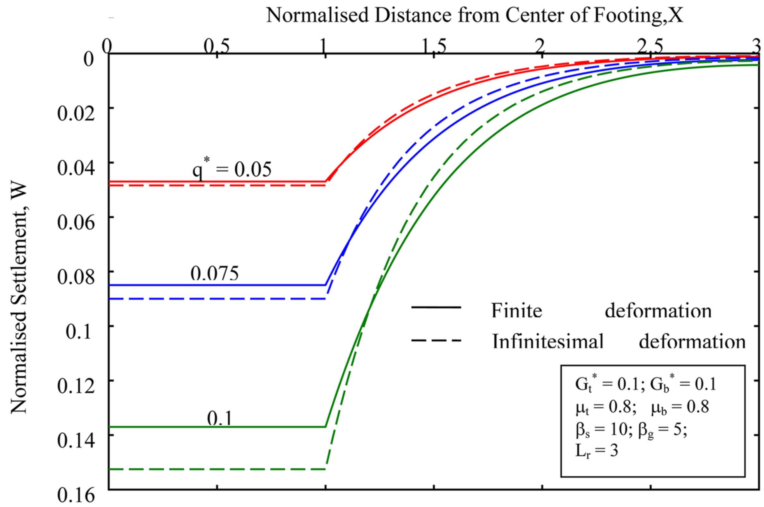

Fig. 7 Settlement profile along the reinforced bed at different average intensities of loads: comparison of infinitesimal and finite deformation theories

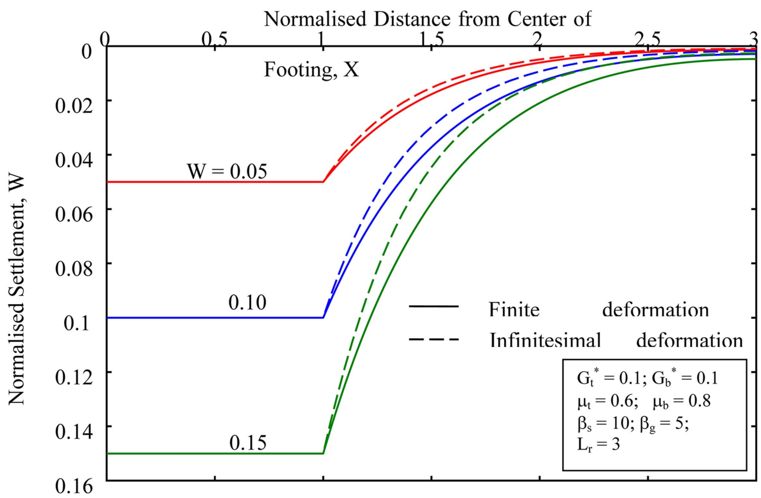

Fig. 8 Settlement profile along the reinforced bed at different footing settlements: comparison of infinitesimal and finite deformation theories

infinitesimal and finite deformation methods are presented in Fig. 7, for an average intensities of loads, $q^* = 0.05$, 0.075 and 0.1 and for shear stiffnesses of the fill above and below reinforcement, $G_t^* = G_b^* = 0.1$, $\beta_s = 10$, $\beta_g = 5$, $q^* = 0.1$ and $\mu_t = \mu_b = 0.8$. The rigid footing settles more according to the infinitesimal theory compared with that by the finite deformation theory for all intensities of load, q^*. This result follows from the basic premise of finite deformation theory according to which (Eqs. 7 and 8) the shear strain is non-linearly related to the derivative of displacement unlike in the infinitesimal theory wherein they are linearly related. The difference between the settlements under the rigid footing by the infinitesimal and the finite deformation theories increases with increasing average intensity of the load, q^*, as the non-linearity effect is more with increasing load. The opposite effect of the settlements by infinitesimal approach being less than those according to finite deformation theory is discernable outside the footing width since equilibrium of forces dictates that the stresses outside the footing width should be lesser than those from finite deformation theory to compensate for the larger ones under the footing width.

Fig. 8 shows the settlement profiles of the reinforced sand bed by the both infinitesimal and finite deformation theories for settlements, $W = 0.05$, 0.1 and 0.15 for shear stiffness of the fill, $G_t^* = G_b^* = 0.1$, $\beta_s = 10$, $\beta_g = 5$, $q^* = 0.1$ and $\mu_t = \mu_b = 0.8$. For any settlement, W, of the footing, the settlement profile beyond the footing width by the infinitesimal theory lies always above the settlement profile by the finite deformation theory indicating lesser settlement. While the settlements of the footing are the same for both finite and infinitesimal approaches, the corresponding loads or average stresses would be different. Thus for a given settlement, W, the footing according to finite deformation theory transmits higher load or average stress than the one according to infinitesimal theory, the difference between these loads increasing with increasing settlements.

The effect of shear stiffness, G_t^*, on settlement profiles of the reinforced foundation bed beneath a rigid footing is studied in Fig. 9 for $G_b^* = 0.1$, $\beta_s = 10$, $\beta_g = 5$, $q^* = 0.1$ and $\mu_t = \mu_b = 0.8$. For an intensity of load, $q^* = 0.1$, the normalised settlement reduces from 0.154 to 0.09, a 41.6% reduction under the rigid footing and increases from 0.0024 to 0.118, a 652% increase, at the edge of the reinforced bed for a ten fold increase of shear stiffness of the granular fill from 0.05 to 0.5. The

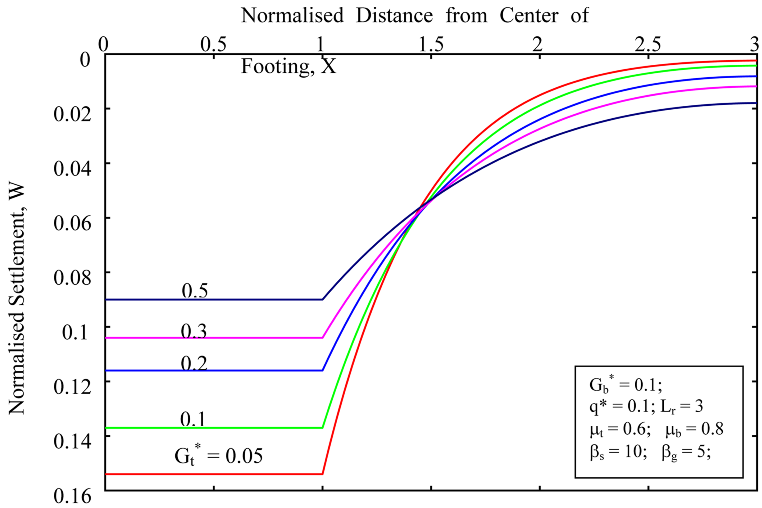

Fig. 9 Variation of settlement with distance along half-width of the reinforced bed: effect of G_t^*

settlements under the footing decrease while settlements outside of the footing increase with increase of relative shear stiffness of the granular fill. Stiff granular fill distributes the load uniformly with larger percentage of the applied load being distributed to outside the loaded region, resulting in an increase of settlement therein while decreasing the settlement under the loaded region. The slopes of the settlement profiles beyond the loaded region also decrease with increasing shear stiffness, G_t^*, of the fill, indicating that the loads are distributed more uniformly with increasing shear stiffness of the granular fill.

The variation of mobilized tension in the reinforcement with distance as effected by shear stiffness, G_t^*, of the fill above the reinforcement is presented in Fig. 10, for relative shear stiffness, $G_b^* = 0.1$,

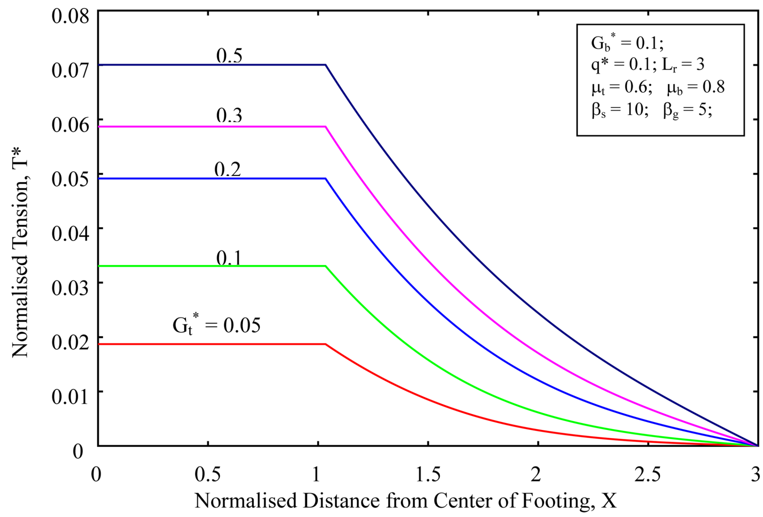

Fig. 10 Variation of mobilized tension with distance along half-width of the reinforced bed: effect of G_t^*

$\beta_s = 10$, $\beta_g = 5$, $q^* = 0.1$ and $\mu_t = \mu_b = 0.8$. For an intensity of load $q^* = 0.1$, the mobilized tension increases from 0.0187 to 0.07 for a ten fold increase of relative shear stiffness, G_t^*, from 0.05 to 0.5. The mobilized tension remains constant under the rigid footing since the settlements are uniform. The mobilized tension increases with increase in shear stiffness, G_t^*, of the fill since stiff granular fill distributes larger stresses to the region outside the footing resulting in greater normal and tangential stresses on the reinforcement leading to an increase in the mobilized tension.

The effect of the ultimate bearing capacity, q_u, of the soft soil on the settlement profile is studied (Fig. 11) through the parameter, β_s $(= k_s B/q_u)$, for $G_t^* = G_b^* = 0.1$, $\beta_g = 5$, $\mu_t = \mu_b = 0.8$. Softer the soil, smaller the ultimate bearing capacity and larger are the values of β_s. The normalised settlements under the rigid footing and at the edge of the reinforced bed for $q^* = 0.1$ increase from 0.096 to

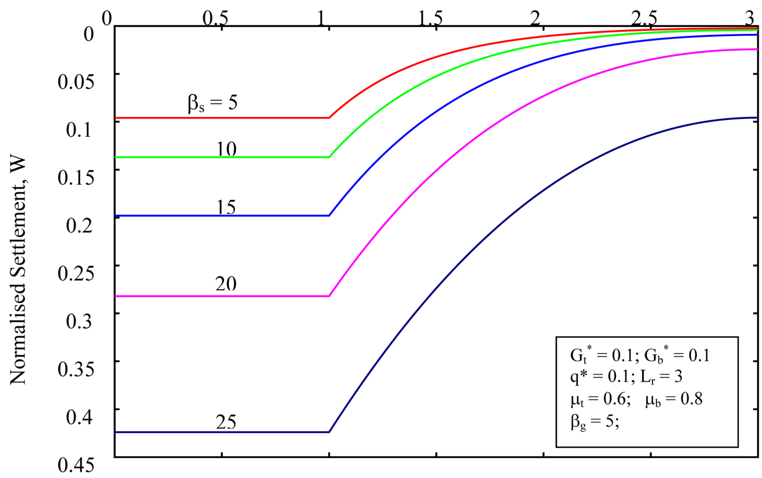

Fig. 11 Variation of settlement with distance along half-width of the reinforced bed: effect of β_s

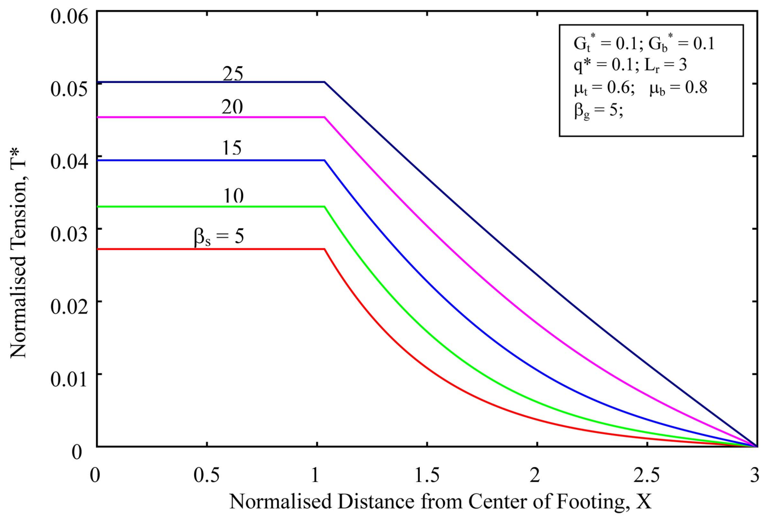

Fig. 12 Variation of mobilized tension with distance along half-width of the reinforced bed: effect of β_s

0.424 and from 0.0023 to 0.0958 respectively for β_s increasing from 5 to 25, *i.e.* from a strong to a soft soil. q^* of 0.1 corresponds to relatively higher percentage of the ultimate bearing stress for increasing values of β_s and hence the settlements increase with β_s.

The variation of tension in the reinforcement with distance with increasing values of β_s is presented in Fig. 12 for $G_t^* = G_b^* = 0.1$, $\beta_g = 5$, $\mu_t = \mu_b = 0.8$ and $q^* = 0.1$. Softer the soil, larger the total and differential settlements and greater the shear strains as depicted in Fig. 11. Thus the increase in β_s results in more shear stresses to be developed for constant shear stiffness of the fill resulting in increase of normal and tangential stresses on the interface of the reinforcement leading to increase in mobilized tension. The normalised tensions thus are 0.027, 0.033, 0.039, 0.045 and 0.050 respectively at the edge of the loaded region for $\beta_s = 5$, 10, 15, 20 and 25. The mobilized tension decreases linearly with distance for higher values of β_s (= 25) and relatively sharply for low values of β_s (= 5) indicating the spread of displacements with distance.

Five (5, 10, 20, 30 and 50) values of the parameter, β_g, are considered in this study of settlement profiles (Fig. 13) with $G_t^* = G_b^* = 0.1$, $\beta_s = 10$, $q^* = 0.1$ and $\mu_t = \mu_b = 0.8$. An increase in β_g implies decrease in the ultimate shear strength of the granular fill since the shear stiffness of the fill is kept constant. The settlement outside the loaded region reduces while the settlement under the loaded region increases with decrease in the shear resistance of the granular fill, *i.e.*, increase in values of β_g. The slope of the settlement profile increases at the edge of the loaded region with increase in β_g, indicating punching mode of failure which occurs when the granular fill is relatively soft and thus fails in shear. The normalised settlement increases from 0.137 to 0.462, a 237.2% increase under the rigid loading and decreases from 0.00425 to 0.0008 (81.2% decrease) at the edge of the reinforced foundation bed with the increase in β_g from 5 to 50, a ten-fold increase. The increase in β_g results in a decrease in the stresses transferred to the fill outside the loaded region. The settlement profile for a high value of the shear parameter, β_g, of 50, indicates punching mode of deformation as the granular fill can not transfer any significant amount of load to the ground outside the rigid footing.

Fig. 14 shows the effect of ultimate shear resistance of the granular fill on the mobilized tension in the reinforcement through β_g values of 5, 10, 20, 30 and 50 for $G_t^* = G_b^* = 0.1$, $\beta_s = 10$, $\mu_t = \mu_b = 0.8$ and $q^* = 0.1$. The normalised tension at the edge of the loaded region increases from 0.033 to

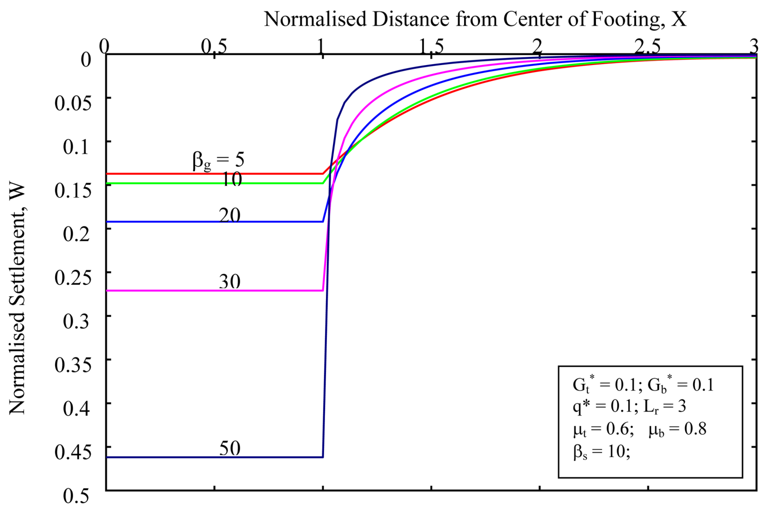

Fig. 13 Variation of settlement with distance along half-width of the reinforced bed: effect of β_g

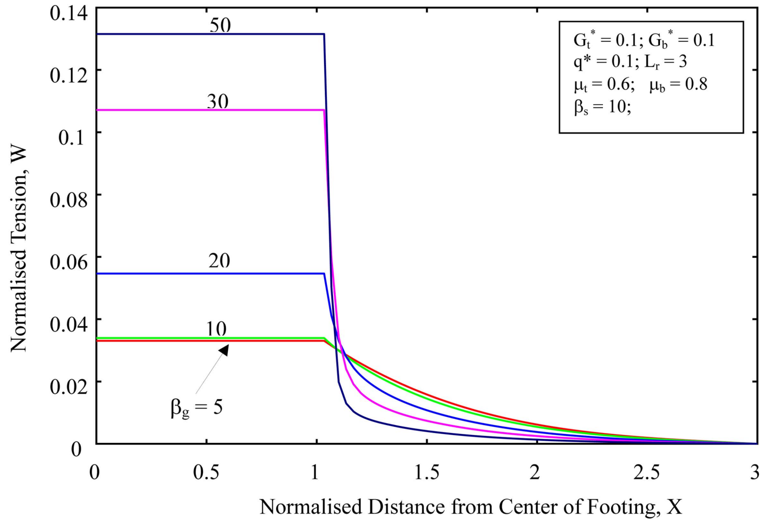

Fig. 14 Variation of mobilized tension with distance along half-width of the reinforced bed: effect of β_g

0.131 for a tenfold increase in β_g from 5 to 50. The settlement profile indicates increasing tendency for punching mode of failure causing an increase in tension in the reinforcement with granular fill having lesser ultimate shear resistance, *i.e.* higher values of β_g. The reinforcement is thus more effective in relatively softer granular fills.

5.1 Load-settlement response

The load-settlement responses of rigid footings on reinforced sand bed overlying soft clay, for shear stiffness, $G_t^* = 0.05$, 0.1, 0.2, 0.3 and 0.5 of the fill above the reinforcement are presented in the Fig. 15 for $G_b^* = 0.1$, $\mu_t = 0.8$, $\mu_b = 0.8$, $\beta_s = 10$ and $\beta_g = 5$. A linear q^* versus W_0 response is

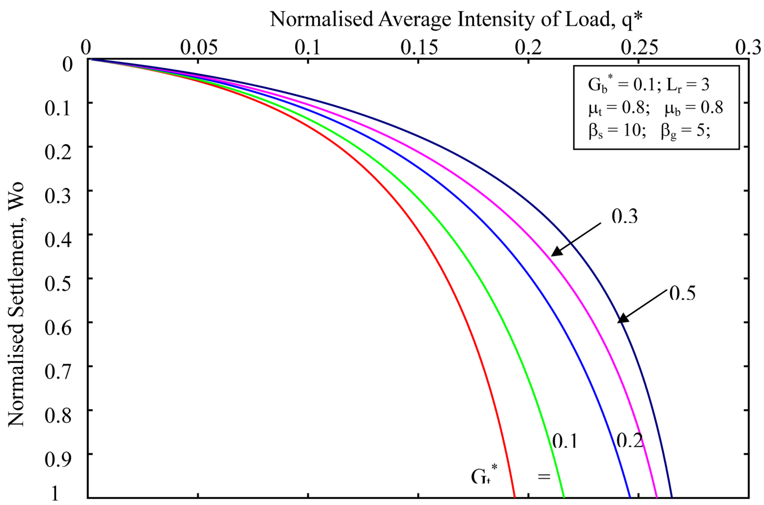

Fig. 15 Intensity of load, q^*-settlement, W_0 responses: effect of G_t^*

exhibited initially by all the curves, the linearity extending to larger applied stresses with increasing values of shear stiffness, G_t^*, of the granular fill. The ultimate or failure loads on the footings increase with increasing shear stiffness, G_t^*, of granular fill, a result similar to that reported by Das (1989). The ability of the granular fill to distribute the applied load over a larger width can be deduced from the results presented. At a normalised settlement of 0.25*B*, the intensities of load, q^*, are 0.126, 0.135, 0.151, 0.163, and 0.179 for G_t^* values of 0.05, 0.1, 0.2, 0.3 and 0.5 respectively. Thus the ultimate bearing capacity of a footing on reinforced granular bed increases with increasing shear stiffness of the granular bed, a result predicted by Meyerhoff (1974) and Meyerhoff and Hanna (1978).

The variation of mobilized maximum tension, T_0^*, with intensity of load, q^*, shown in Fig. 16, exhibits some interesting phenomenon. In all the cases, T_0^*, initially increases linearly with applied average stress, q^*. However, the rate of increase of T_0^* with q^* increases with decrease in G_t^*. Softer the granular fill, the smaller would be the stresses carried by the granular fill especially at larger loads. The mobilized tensions are respectively 0.0259, 0.0521, 0.0894, 0.115 and 0.149 for G_t^* = 0.05, 0.1, 0.2, 0.3 and 0.5 and for the intensity of load, q^* = 0.3. The values of tension increase with G_t^*, because the stiff granular fill transfers more stresses to the fill beyond the footing causing more normal and shear stresses to be mobilized at the interface of the fill and the reinforcement, resulting in larger mobilized tensions in the reinforcement.

The parameter, β_s, signifying the influence of the undrained strength, c_u, or the ultimate bearing capacity, q_u, has a significant effect (Fig. 17) on the normalized load versus settlement responses. For low values of the ultimate bearing capacity of the soft ground, q_u, *i.e.* high values of β_s, (> 20), low ultimate footing pressures are attained with the settlements increasing very sharply. At a normalized settlement of 0.1*B*, the intensities of load, q^*, are 0.103, 0.0833, 0.0623, 0.0509, and 0.0383 for values of β_s 5, 10, 20, 30 and 50 respectively. The load-settlement response curves shifts towards the right with increasing values of β_s, indicating decrease in settlement for the same average intensity of load, q^*.

The maximum mobilized tension in the reinforcement varies (Fig. 18) with the ultimate bearing

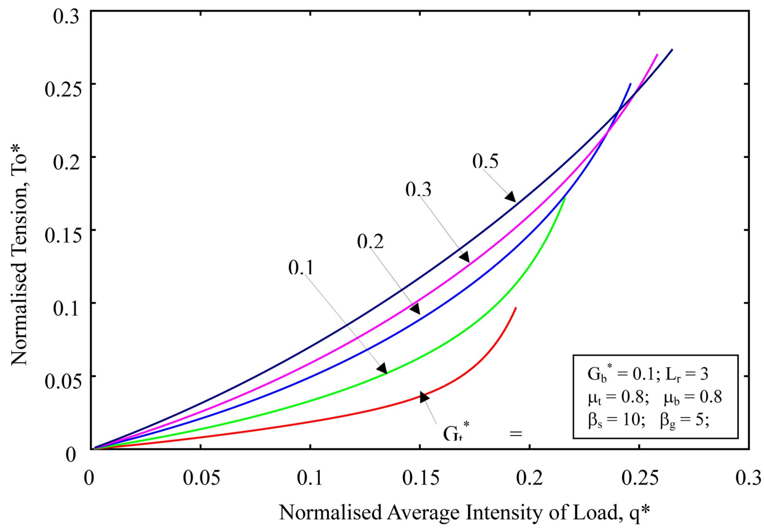

Fig. 16 Intensity of load, q^*-tension, T_0, responses: effect of G_t^*

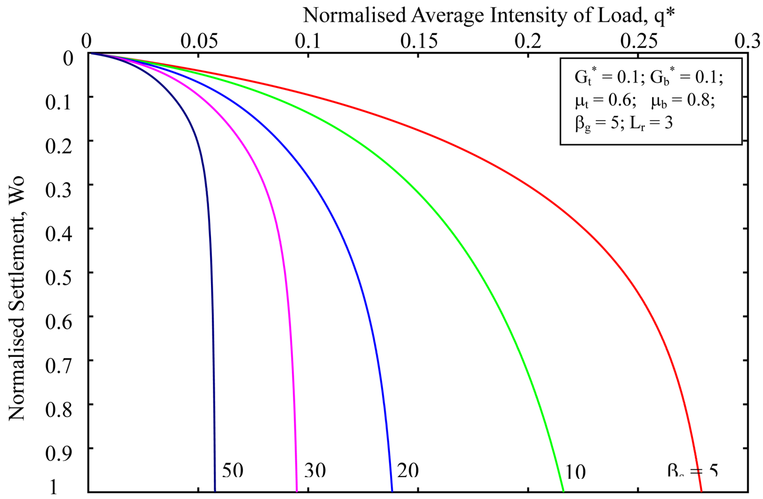

Fig. 17 Intensity of load, q^*-settlement, W_0, responses: effect of β_s

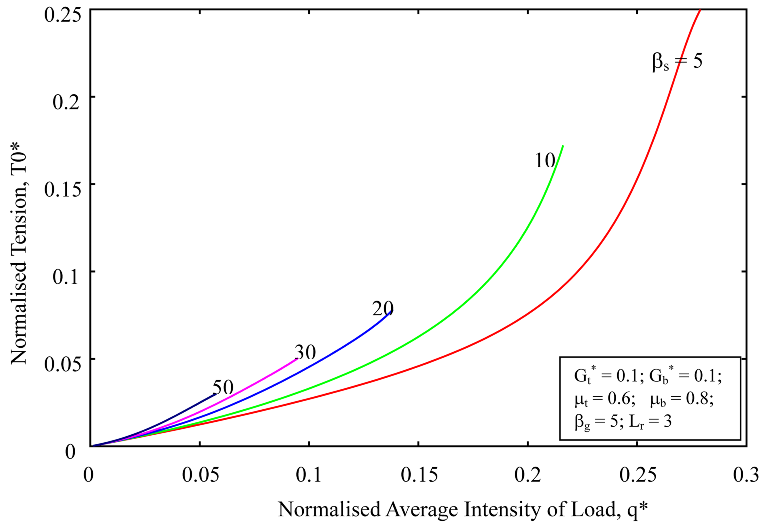

Fig. 18 Intensity of load, q^*-tension, T_0, responses: effect of β_s

capacity, q_s, of the soft soil, for $\beta_s = 5$, 10, 20, 30 and 50 and for $G_t^* = G_b^* = 0.1$ and $\beta_g = 5$. Mobilized tension in the reinforcement increases with increase in β_s, since as the ultimate bearing capacity, q_u, of the soft soil decreases, it causes larger settlements (Fig. 17) leading to larger tensions to be mobilized in the reinforcement. The mobilized tensions are respectively 0.0282, 0.0258, 0.0225, 0.0202 and 0.0170 for $\beta_s = 5$, 10, 20, 30 and 50 at settlement, $W_0 = 0.1$.

The influence of ultimate shear resistance, τ_f, of the granular fill on the intensity of load-settlement responses of the rigid footing for the $\beta_g = 5$, 10, 20, 30, and 50 is presented in the Fig. 19 for $G_t^* = G_b^* = 0.1$ and $\beta_s = 50$. The intensity of load-settlement response curves for soft granular fills, *i.e.*, for larger values of β_g, indicate once again a punching mode of failure while stronger fills indicate a continuous increase in q^* with settlement, W. An increase in β_g $(= G_s/\tau_f)$ implies a

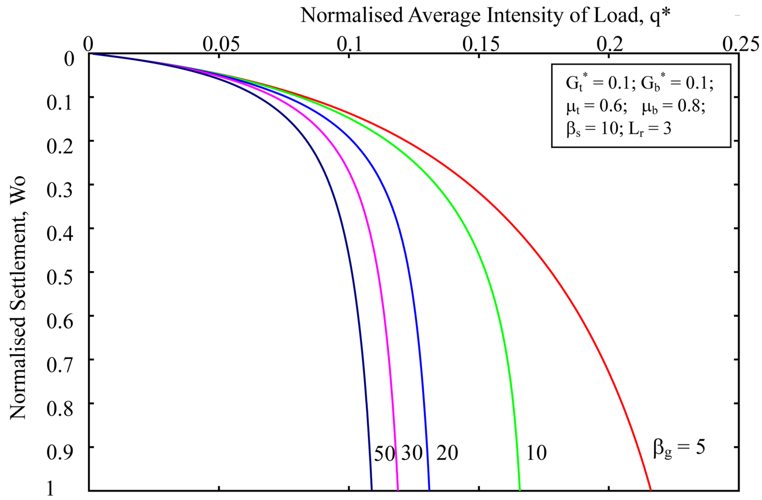

Fig. 19 Intensity of load, q^*-settlement, W_0, responses: effect of β_g

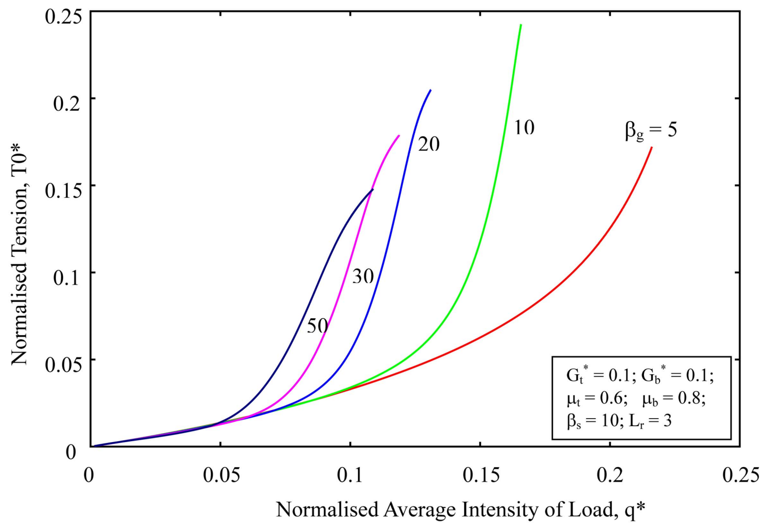

Fig. 20 Intensity of load, q^*-tension, T_0, responses: effect of β_g

decrease in ultimate shear resistance, τ_f, of the granular fill, that is, the granular fill is weak. Hence its capability to distribute the loads more widely reduces causing the increases in settlements. For settlement equal to 10% of B, the intensities of load are 0.0651, 0.0715, 0.0761, 0.0812 and 0.0833 for β_g equal to 50, 30, 20, 10 and 5 respectively.

The intensity of load-maximum mobilized tension responses of the footing for $\beta_g = 5$, 10, 20, 30 and 50 are presented in the Fig. 20 for $G_t^* = G_b^* = 0.1$ and $\beta_s = 10$. All the curves merge at low stress levels but deviate from linearity with approaching failure stress. The differential settlements increase towards failure leading to larger shear strains and larger shear stresses in the granular fill and higher tension in the reinforcement. Granular beds with increasing values of β_g, fail by punching at low bearing stresses resulting in high values of normalised maximum tension at smaller loads. The mobilized tensions are respectively 0.0225, 0.0236, 0.0248, 0.0252 and 0.0311 for $\beta_g = 5$, 10, 20, 30 and 50 and for the intensity of load, $q^* = 0.1$. Mobilized tension is more for stronger granular fills and correspond to higher bearing stresses.

6. Conclusions

In the present paper, a finite deformation theory is proposed for the analysis and study of the response of a rigid footing on a reinforced foundation bed incorporating non-linear stress-displacement response of super soft soil and non-linear shear stress-shear strain response of granular fill. The model consists of Pasternak shear layer, rough membrane and elasto-plastic Winkler springs to represent the granular fill, the reinforcement layer and the super-soft soil respectively. Full interfacial friction, μ, (= tan ϕ) is assumed to be mobilized at the top and the bottom faces of the reinforcement. Parametric study carried out highlights the results of the finite deformation theory and quantifies the effects of all the relevant parameters on the settlement response of a rigid footing.

The normalised average intensity of load increase by about 41% with increase of shear stiffness, G_t^* from 0.05 to 0.5 at footing settlement equal to 25%B. For a ten fold (from 5 to 50) increase in non-linear parameter, β_s, the normalized average intensity of load decreases by about 63% at normalized rigid settlement equal to 0.1B. The normalized average intensity of load decreases by about 22% for a ten fold increase in β_g, (from 5 to 50) at normalized rigid settlement equal to 10%B. The influence of frictional resistance at the interface (μ_t and μ_b) on the average intensity of load is very less and is equal to only 3% increase for an increase in μ_t and μ_b from 0.3 to 1.0.

References

Akinmusuru, J.O. and Akinbolade, J.A. (1981), "Stability of loaded areas on reinforced soil", *J. Geotech. Eng. Division - ASCE*, **107**(6), 819-827.

Andrawes, K.Z., McGown, A. and Wilson-Fahmy, R.F. (1983), "The behaviour of a geotextile reinforced sand loaded by a strip footing", *Proc. of 8th Europian Conference on Soil Mechanics and Foundation Engineering*, Helsinki, **1**, 329-334.

Basset, R.H. and Last, N.C. (1978), "Reinforcing earth below footings and embankments", *Proc. Symp. Earth Reinforcement - ASCE*, **101**, 1241-1255.

Binquet, J. and Lee, K.L. (1975a), "Bearing capacity tests on reinforced earth slabs", *J. Geotech. Eng. - ASCE*, **101**(12), 1241-1255.

Binquet, J. and Lee, K.L. (1975b), "Bearing capacity analysis of reinforced earth slabs", *J. Geotech. Eng. Division - ASCE*, **101**(12), 1257-1276.

Das, B.M. (1989), "Foundation on sand underlain by soft clay with geotextile at sand-clay interface", *In Geosynthetics, '89 Conference*, Sandiego, USA, **1**, 203-214.

Dembicki, E., Jermolowicz, P. and Niemunis, A. (1986), "Bearing capacity of strip foundation on soft soil reinforced by geotextile", *Proc. of 3rd International Conference on Geotextiles*, Vienna, Austria, **1**, 205-209.

Ghosh, C. and Madhav, M.R. (1994a), "Settlement response of reinforced shallow earth bed", *Geotext. Geomembranes*, **13**(5), 643-656.

Guido, V.A., Biesiadecki, G.L. and Sullivan, M.J. (1985), "Bearing capacity of a geotextile reinforced foundation", *Proc. of 11th International Conference on Soil Mechanics and Foundation Engineering*, San Francisco, **3**, 1777-1780.

Guido, V.A., Chang, D.K. and Sweeny, M.A. (1986), "Comparison of geogrid and geotextile reinforced earth

slabs", *Can. Geotech. J.*, **23**(4), 435-440.
Love, J.P., Burd, H.J., Milligan, G.W.E. and Houlsby, G.T. (1987), "Analytical and model studies of reinforcement of a layer of granular fill on a soft clay subgrade", *Can. Geotech. J.*, **24**(4), 611-622.
Madhav, M.R. and Poorooshasb, H.B. (1988), "A new model for geosynthetic reinforced soil", *Comput. Geotech*, **6**(4), 277-290.
Maheshwari, P., Basudhar P.K. and Chandra, S. (2006), "Modeling of beams on reinforced granular beds", *Geotech. Geol. Eng.*, **24**(2), 313-324.
Meyerhof, G.G. (1974), "Ultimate bearing capacity of footings on sand layer overlying clay", *Can. Geotech. J.*, **11**(2), 224-229.
Meyerhof, G.G. and Henna, A.M. (1978), 'Ultimate bearing capacity of foundations on layered soil under inclined load", *Can. Geotech. J.*, **15**(4), 565-572.
Milligan, G.W.E., Fannin, J. and Farrar, D.M. (1986), "Model and full-scale tests of granular layers reinforced with a geogrid", *Proc. of 3rd International Conference on Geotextiles*, Vienna, Austria, 61-66.
Purkayastha, R.D. and Bhaumik, M.K. (1988), "Performance of geogrid and geotextile below foundation on soft soil", *Proc. of Indian Goetechnical Conference*, Allahabad, December, **1**, 199-204.
Ramu, K. (2001), "Modelling approaches for and analysis of reclamation process and response of reclaimed ground", *Ph.D. Dissertation,* Indian Institute of Technology, Kanpur, India.
Terzaghi, K. (1955), "Evaluation of coefficients of subgrade reaction", *Geotechnique*, **5**(4), 297-326.
Saran, S., Rao, A.S.R. and Singh, H. (1985), "Behaviour of eccentrically loaded footings on reinforced earth slab", *Proc. of Indian geotechnical Conference*, Roorkee, **1**, 177-122.
Shukla, S.K. and Chandra, S. (1994), "The effect of prestressing on the settlement characteristics of geosynthetic reinforced soil", *Geotext. Geomembranes*, **13**, 531-543.
Yang, Z. (1972), "Strength and deformation characteristics of reinforced sand", *Ph.D, Dissertation*, University of California at Los Angeles.
Yin, J.H. (1997a), "Modelling geosynthetic reinforced granular fills over soft soil", *Geosynth. Int.*, **4**(2), 165-185.
Yin, J.H. (1997b), "A nonlinear model of geosynthetic-reinforced granular fill over soft soil", *Geosynth. Int.*, **4**(5), 523-537.

PL